Bioorganic & Medicinal Chemistry 18 (2010) 4485–4497

Contents lists available at ScienceDirect

Bioorganic & Medicinal Chemistry

journal homepage: www.elsevier.com/locate/bmc

ppGpp analogues inhibit synthetase activity of Rel proteins from Gram-negative and Gram-positive bacteria

Ezequiel Wexselblatt [a], Jehoshua Katzhendler [a,*], Raspudin Saleem-Batcha [b], Guido Hansen [b], Rolf Hilgenfeld [b], Gad Glaser [c], Roee R. Vidavski [c]

[a] The Institute for Drug Research, School of Pharmacy, The Hebrew University of Jerusalem, Room 414, Jerusalem 91120, Israel
[b] Institute of Biochemistry, Center for Structural and Cell Biology in Medicine, University of Lübeck, Lübeck, Germany
[c] Institute for Medical Research Israel-Canada, Department of Developmental Biology and Cancer Research, Hebrew University of Jerusalem, Jerusalem, Israel

ARTICLE INFO

Article history:
Received 14 January 2010
Revised 20 April 2010
Accepted 21 April 2010
Available online 28 April 2010

Keywords:
ppGpp
RelA
Stringent response
Antibacterial

ABSTRACT

A prominent feature of the stringent response is the accumulation of two unusual phosphorylated derivatives of GTP and GDP (pppGpp: 5′-triphosphate-3′-diphosphate, and ppGpp: 5′-3′-bis-diphosphate), collectively called (p)ppGpp, within a few seconds after the onset of amino-acid starvation. The synthesis of these 'alarmone' compounds is catalyzed by RelA homologues. Other features of the stringent response include inhibition of stable RNA synthesis and modulation of transcription, replication, and translation. (p)ppGpp accumulation is important for virulence induction, differentiation and antibiotic resistance. We have synthesized a group of (p)ppGpp analogues and tested them as competitive inhibitors of Rel proteins in vitro. 2′-Deoxyguanosine-3′-5′-di(methylene bisphosphonate) [compound (**10**)] was found as an inhibitor that reduces ppGpp formation in both Gram-negative and Gram-positive bacteria. In silico docking together with competitive inhibition analysis suggests that compound (**10**) inhibits activity of Rel proteins by competing with GTP/GDP for its binding site.
As Rel proteins are completely absent in mammalians, this appears to be a very attractive approach for the development of novel antibacterial agents.

1. Introduction

The need for new antibiotic drugs with novel targets has been recognized by health organizations, industry and academia alike.[1] At present, most of the drugs administered to treat bacterial infections are aimed to one of the following four processes: protein synthesis, nucleic-acid synthesis, cell-wall synthesis, or folate synthesis.[2] Due to the extensive knowledge accumulated in the field, substantial efforts have been implemented to interfere with these essential synthetic pathways. Careful examination of other processes in bacteria revealed that targeting the stringent response has potential to lead to the development of a novel class of antibacterial agents.

The pleiotropic response, called the 'stringent response', was initially described for *Escherichia coli* cells more than 40 years ago.[3] The first observed feature of the stringent response was the intracellular accumulation of guanosine tetraphosphate (ppGpp) and guanosine pentaphosphate (pppGpp) (collectively known as (p)ppGpp or 'alarmones') within a few seconds after the advent of amino-acid starvation.[4,5] Other features of the stringent response include inhibition of stable RNA synthesis and changes in essential processes, namely, transcription, replication and translation.[3,6] In addition, (p)ppGpp accumulation was also found to be important for virulence induction,[7–12] differentiation,[13] and development of antibiotic resistance.[14]

In *E. coli*, the mutation causing the relaxed phenotype, which fails to accumulate (p)ppGpp during amino-acid starvation, was mapped to the *relA* gene which encodes a 84-kDa protein, RelA.[15] RelA is a ribosome-associated (p)ppGpp synthetase that is activated in response to amino-acid starvation.[3] During amino-acid starvation, the binding of uncharged tRNAs to the ribosomal 'A' site stalls protein synthesis, stimulating a reaction in which RelA transfers a pyrophosphoryl group comprising the β- and γ-phosphates of an ATP donor to the 3′-hydroxy group of GTP or GDP to form pppGpp and ppGpp, respectively.[3] In cell extracts, RelA is found to be associated only with a small fraction of the ribosomes (about 1%).[16] Despite this low abundance of RelA, up to mM levels of (p)ppGpp are rapidly produced. This is feasible since (p)ppGpp synthesis evokes dissociation of RelA from the ribosome, allowing the enzyme to shuttle to another stalled ribosome and repeat the reaction.[17]

In addition to amino-acid starvation, (p)ppGpp synthesis in Gram-negative bacteria can be induced by other stress conditions such as deprivation of phosphorus, iron, carbon source, and fatty acids in a SpoT-dependent mode.[3,18–20] Equally important, SpoT

* Corresponding author. Tel.: +972 2 6758693; fax: +972 2 6757076.
E-mail address: katzhe@cc.huji.ac.il (J. Katzhendler).

0968-0896/$ - see front matter © 2010 Elsevier Ltd. All rights reserved.
doi:10.1016/j.bmc.2010.04.064

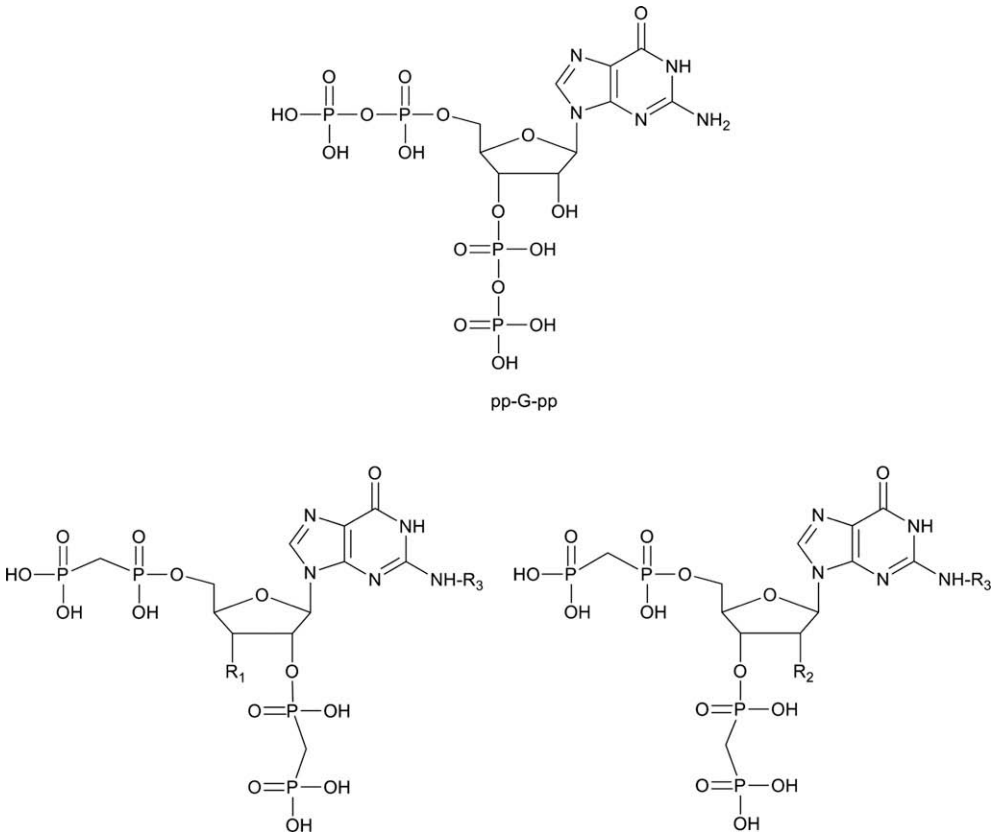

Figure 1. ppGpp and its pcpGpcp analogues **5a**: R_1 = OH, R_3 = *i*bu; **5b**: R_2 = OH, R_3 = *i*bu; **5c**: R_1 = OTBDMS, R_3 = *i*bu; **5d**: R_2 = OTBDMS, R_3 = *i*bu; **6a**: R_1 = OH, R_3 = H **6b**: R_2 = OH, R_3 = H; 10: R_2,R_3 = H.

also acts as a ribosome-independent (p)ppGpp hydrolase that degrades (p)ppGpp to GDP/GTP and pyrophosphate.[21] Residual (p)ppGpp synthesis found in Δ*relA* is abolished in a Δ*relA*Δ*spoT* ('double null') mutant.[22] Cells with this double deletion show a complex phenotype that includes loss of ability to grow on amino-acid-free minimal medium and morphological alterations.[22] It was also verified that Gram-positive bacteria, which lack SpoT homologues, have a RelA homologue with both (p)ppGpp-synthetase and (p)ppGpp-hydrolase activities.[23–25] Deletion of the *relA-spoT* integrated gene in the Gram-positive *Bacillus subtilis* was thought to generate a phenotype resembling that of 'double null' in *E. coli*.[25] However, recently two additional factors (YjbM and YwaC) were found to have (p)ppGpp-synthetase activity in *B. subtilis*.[26] Molecular genetic analysis revealed that *ywaC* is induced by alkaline shock and it has been suggested that both YjbM and YwaC might have more specialized functions in (p)ppGpp metabolism.

Recently, the crystal structure of the catalytic N-terminal fragment (NTD, residues 1–385, termed Rel*seq*385) of the bifunctional RelA homologue from the Gram-positive bacterium *Streptococcus equisimilis* was determined at 2.1 Å resolution.[27] In contrast to Gram-negative bacteria, where RelA and SpoT are distinct proteins, this fragment displays both the hydrolase and synthetase active sites residing more than 30 Å apart from each other. Futile recycling of the substrate is avoided by a complex regulatory mechanism that involves subtle conformational changes in the protein. The crystallographic analysis revealed two conformations for Rel*seq*385 that, respectively, typify the opposing hydrolase-OFF/synthetase-ON and hydrolase-ON/synthetase-OFF states.[27]

The crystal structure also suggested a mechanism for the attack of the 3′-OH group of GDP (or GTP) onto the β-phosphorus atom of ATP. Most likely, Glu323 of Rel*seq*385 activates the hydroxyl group by proton abstraction; it will also coordinate the essential Mg^{2+} ion which is not present in the crystals and is expected to be bound to the pyrophosphate donor, ATP.[27] Support for a critical role of Glu323 in the synthetase mechanism derives from a follow-up mutational study: a Rel*seq*385 mutant bearing a Glu323Gln substitution exhibited severely defective synthetase activity.[27]

In this paper, we report the synthesis of a variety of (p)ppGpp analogues and the study of their inhibitory properties on RelA and its homologue, Rel*seq*385. The compounds include two main features: (1) the pyrophosphate moieties at positions 5′ and 3′ are replaced by non-hydrolyzable methylene-bisphosphonate groups and (2) the sugar moiety consists of either ribose or 2′-deoxyribose. Analogues carrying a methylene-bisphosphonate group at the 2′ position are also reported. Figure 1 depicts the alarmone ppGpp and the schematic structure of the inhibitors bearing double methylene-bisphosphonate substitutions.

2. Results and discussion

2.1. Chemical synthesis

The synthesis of (**5a**), (**5b**), (**6a**) and (**6b**) is outlined in Scheme 1. We have selected the isobutyryl group for the protection of the exocyclic amine. Treatment of guanosine with trimethylsilyl chloride in pyridine as a transient protection of the ribose hydroxyl groups followed by the addition of isobutyric anhydride afforded N^2 *i*bu nucleoside (**1**) in 79% yield. Compound (**1**) was re-crystallized from hot water.

5′-*O*-Dimethoxytritylation of (**1**) gave (**2**) in 73% yield. Compound (**2**) precipitates from a mixture of diethyl ether and petroleum ether (3:1).

Subsequent silylation of the latter with TBDMS (*tert*-butyl dimethyl silyl)[28] resulted in a mixture of positional isomers (**3a**) and (**3b**) that were separated by preparative HPLC on a C18 column

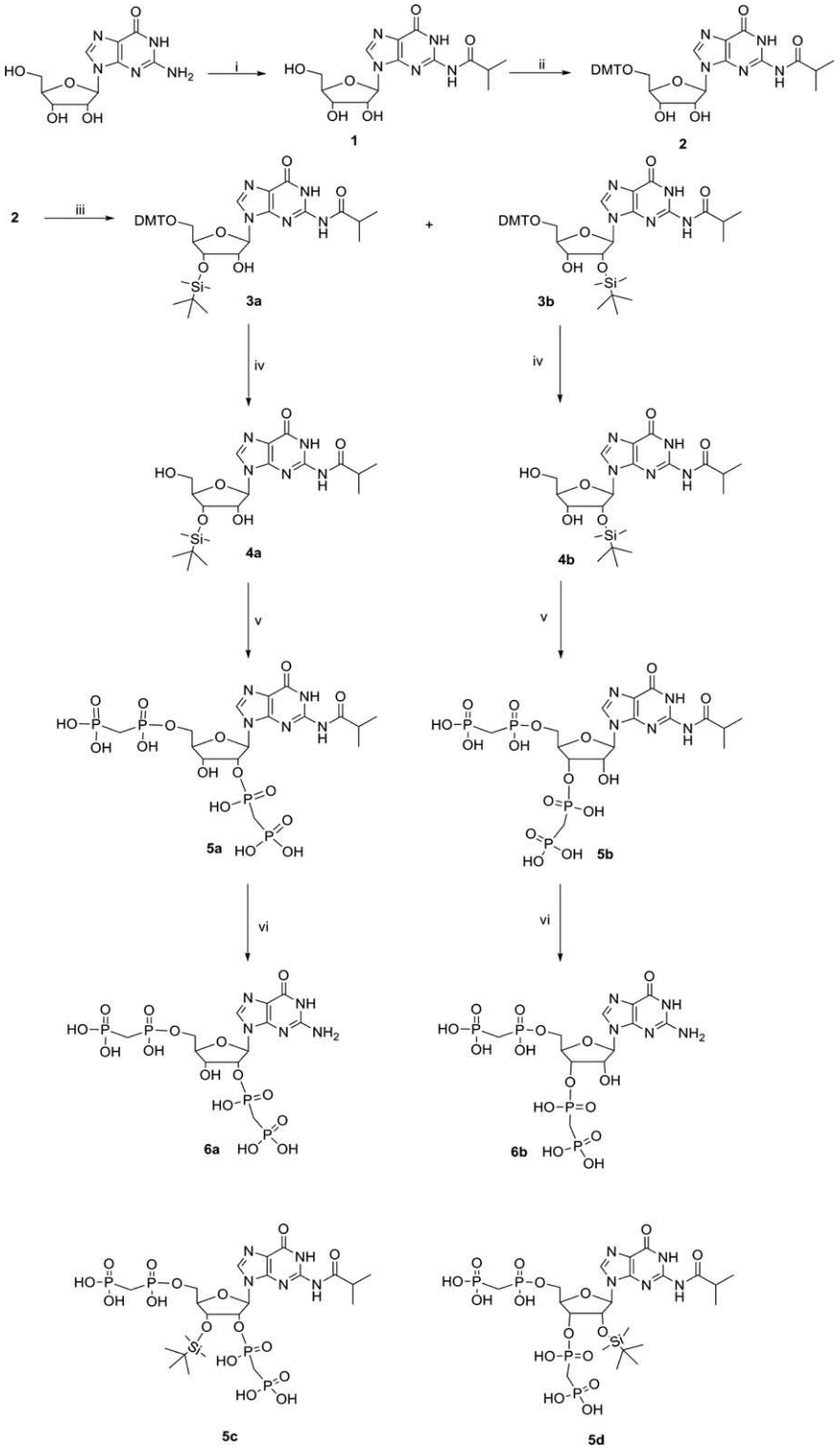

Scheme 1. Reagents and conditions: (i) isobutyric anhydride, pyridine, room temperature, 5 h (79%); (ii) DMT–Cl pyridine, room temperature, 4 h (73%); (iii) TBDMS–Cl, DCM, room temperature, overnight (34–63%); (iv) 5% DCA/DCM, room temperature, 15 min (95%); (v) (a) methylene bis-(phosphonic dichloride), trimethyl phosphate, 0 °C to room temperature, overnight; (b) 0.5 M ammonium bicarbonate, 0 °C, 15 min (44–73%); (vi) ammonium hydroxide, 60 °C, overnight (97%).

employing isocratic elution (70% acetonitrile/water). The products were identified by 2D NMR.

After detritylation of isomers (**3a**) and (**3b**) with 5% dichloroacetic acid (DCA) in methylene chloride (DCM) followed by flash-chromatography purification, the pure products (**4a**) and (**4b**) were then bisphosphonylated (step v) employing methylene-bis-(phosphonic dichloride) in trimethyl phosphate. Upon completion of the phosphonylation, the solution was treated with a concentrated solution of ammonium bicarbonate to afford the di-bisphosphonylated products (**5a**) and (**5b**). Compound (**5b**) precipitated and was isolated by filtration while (**5a**) remained completely soluble in the reaction mixture. The TBDMS protecting group is sensitive to

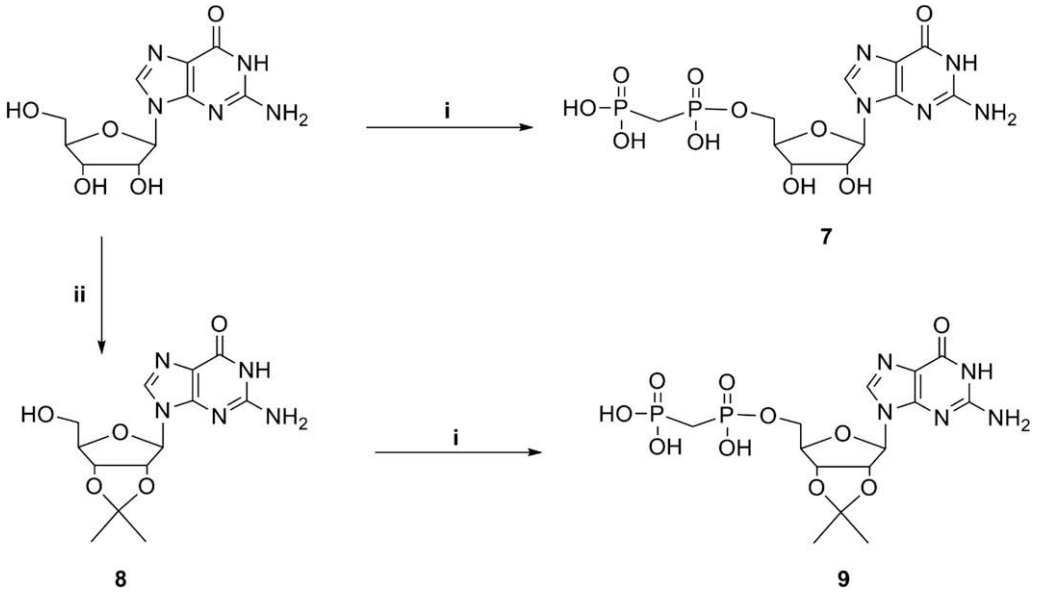

Scheme 2. Reagents and conditions: (i) (a) mMethylene bis-(phosphonic dichloride), trimethyl phosphate, 0 °C to room temperature, 2 h; (b) 0.5 M ammonium bicarbonate, 0 °C, 15 min (67–70%); (ii) acetone, room temperature, 70 min (83%).

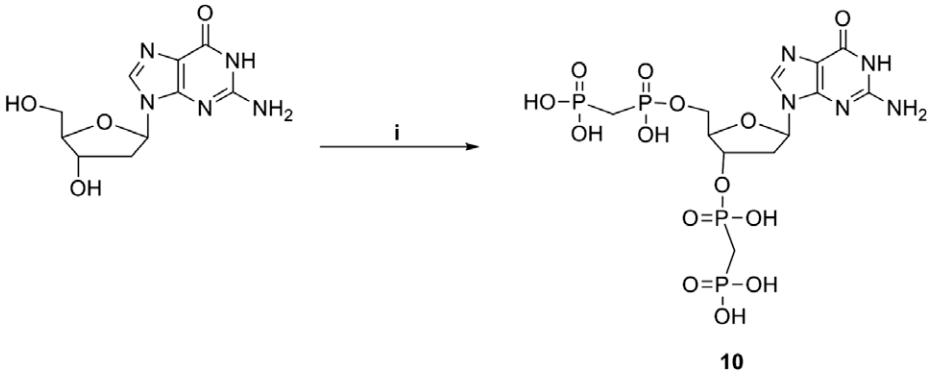

Scheme 3. Reagents and conditions: (i) (a) methylene bis-(phosphonic dichloride), trimethyl phosphate, 0 °C to room temperature, overnight; (b) 0.5 M ammonium bicarbonate, 0 °C, 15 min (73%).

highly acidic conditions and was almost completely removed during the phosphonylation step; a reaction that involves the generation of acidic conditions.

The products were purified on a reverse-phase preparative HPLC system. Peaks were separated and identified by mass spectroscopy. Small amounts of compounds (**5c**) and (**5d**) and traces of the mono-phosphonylated compounds were also detected.

Removal of the isobutyryl protecting group on the exocyclic amine at position 2 of the nucleobase of (**5a**) and (**5b**) was achieved by treating these compounds with concentrated ammonium hydroxide at 60 °C in sealed tubes overnight affording compounds (**6a**) and (**6b**), respectively.

The overall yields (six steps) for (**6a**) and (**6b**) were 8.5% and 13.6%, respectively.

Compounds (**7**) and (**9**) were synthesized by direct phosphonylation with methylene-bis-(phosphonic dichloride) (Scheme 2) starting with guanosine and isopropylidene guanosine, respectively.[29]

The synthesis of **10** followed the same procedure as for (**5a**) and (**5b**) and is depicted in Scheme 3. Thus, the desired product precipitated after the addition of ammonium bicarbonate to form the phosphonic acid. The precipitate was collected and purified in the same manner as described for compounds (**5a)** and (**5b**) affording compound (**10**) in 73% yield.

In addition to the 3′-5′-bis-methylene-bisphosphonate adducts (**6a**) and (**6b**) and to the 5′-bisphosphonate **7**, the 3′-methylene-bisphosphonate derivative was also prepared. The synthetic route for the preparation of deoxyguanosine-3′-yl-bisphosphonate **14** is shown in Scheme 4. In this synthesis, an appropriate protecting group is required for the 5′-OH group. Under the reaction conditions employing trimethyl phosphate as the solvent of choice, HCl evolves. Thus, acid-labile DMT and TBDMS are not stable protecting groups under these reaction conditions. An attempt to add base such as triethylamine or pyridine to the reaction mixture did not lead to the desired product, nor did the use of pyridine as solvent. This is probably due to the role played by trimethylphosphate as described by Yoshikawa et al.[30] Acetyl as protecting group was selected and found to be adequate. 5′-Acetyl-2′-deoxyguanosine was obtained by acylation of 2′-deoxyguanosine with acetic anhydride in dry pyridine. The di-acetylated product was treated with hydrazine hydrate to yield a partial deacetylated mixture.[31] The mixture of 5′-acetyl- and 3′-acetyl-2′-deoxyguanosine was separated on RP-C18 preparative HPLC and the isolated compounds were identified by 2D ^{1}H NMR. Figure 2 displays a typical HPLC chromatogram highlighting the identification of 5′-acetyl-2′-deoxyguanosine. Phosphonylation was carried out as described (vide supra) and the final step of acetyl deprotection was achieved by

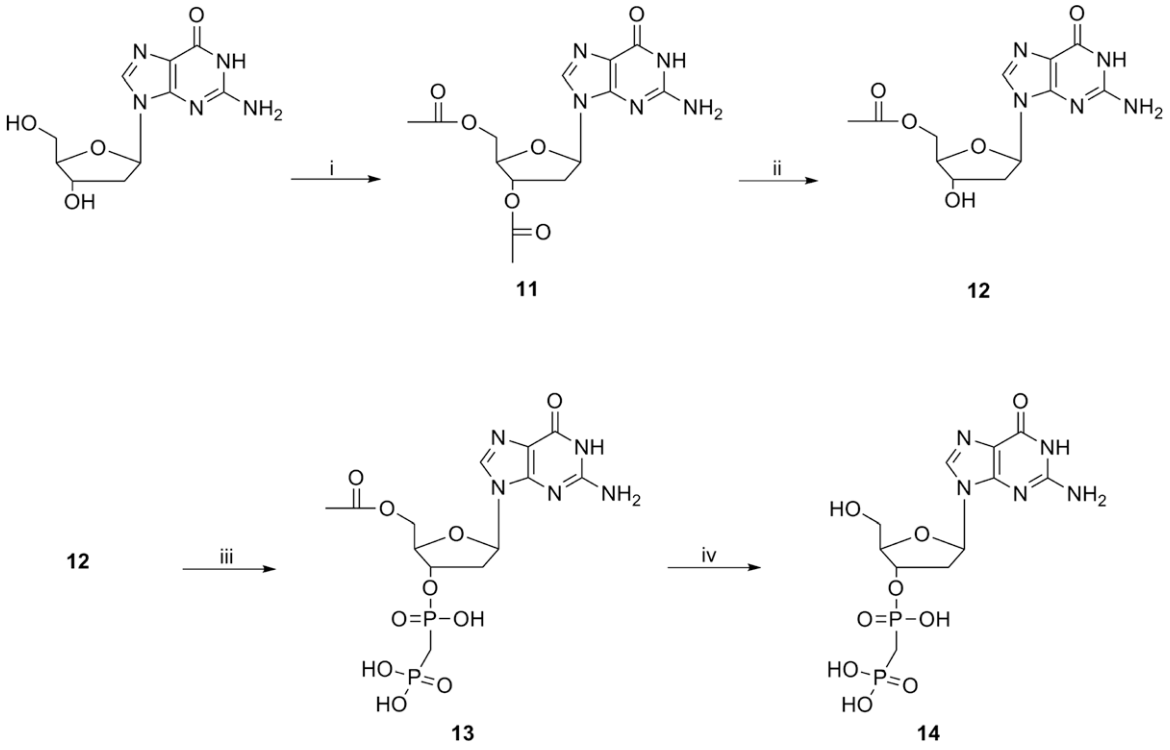

Scheme 4. Synthesis of 3′-bisphosphonyl-2′-deoxyguanosine. Reagents and conditions: (i) acetic anhydride, pyridine, room temperature, 45 min (90%); (ii) $H_2NNH_2{\cdot}H_2O$, pyridine, overnight (47%); (iii) (a) methylene bis-(phosphonic dichloride), trimethyl phosphate, 0 °C to room temperature, overnight; (b) 0.5 M ammonium bicarbonate, 0 °C, 15 min (67%); (iv) ammonium hydroxide, 60 °C, 15 h (91%).

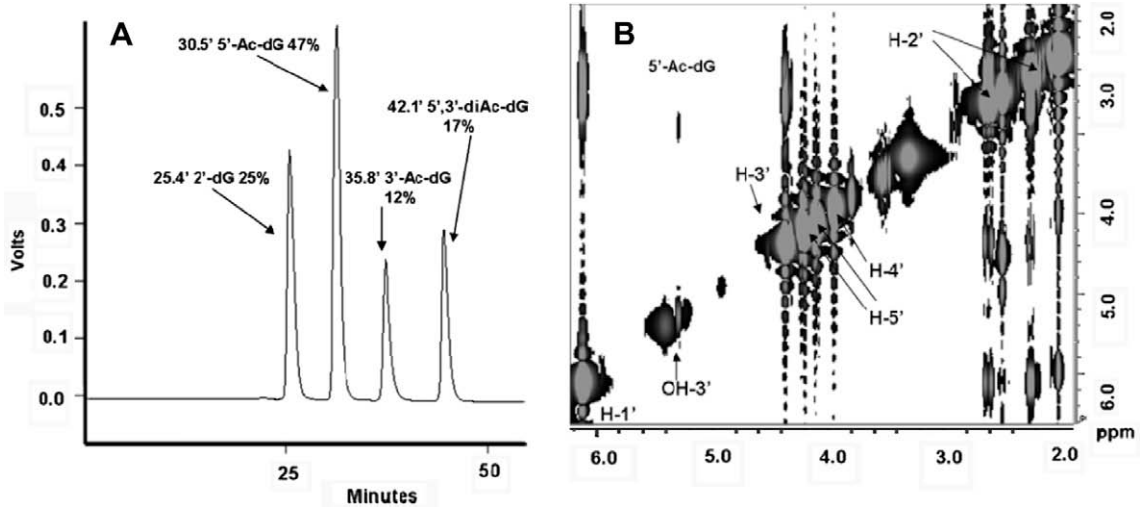

Figure 2. (A) RP-C18 HPLC separation of compound (**12**) using a linear gradient from 0% to 90% acetonitrile in water over 50 min with a flow rate of 5 mL/min. (B) 2D NMR of 5′-acetyl-2′-deoxyguanosine. The triplet signal at 6.18 ppm was identified as 1′H and used as reference for the assignment of the remaining hydrogen atoms of the sugar ring.

treating compound (**13**) with ammonium hydroxide yielding the desired product.

2.2. ppGpp analogues possess the ability to inhibit the synthetic activity of both *E. coli* RelA and Rel*seq*385 in vitro

The biological activity of the synthesized ppGpp analogues was evaluated in vitro (Fig. 3) with *E. coli* RelA and Rel*seq*385. 'RelA' denotes the full-length RelA protein from *E. coli*, comprising the N-terminal domain with (p)ppGpp-synthetase activity and the C-terminal ribosome-binding domain. 'Rel*seq*385' denotes the bifunctional N-terminal domain of the *S. equisimilis* RelA homologue harboring (p)ppGpp-synthetase and hydrolase activities in separate catalytic sites; this recombinant protein construct lacks the C-terminal ribosome-binding domain.

All of the synthesized compounds possess the ability of inhibiting (p)ppGpp accumulation. Furthermore, a dose-response correlation was observed. In general, analogues bearing the bisphosphonate substitution at positions 5′ and 3′ (compounds (**5d**), (**5b**), (**6b**), and (**10**)) show more potent inhibition than others. It can be seen (Fig. 3A) that for these four inhibitors, substitution at the 2′ position plays a role in the inhibitory characteristic of all

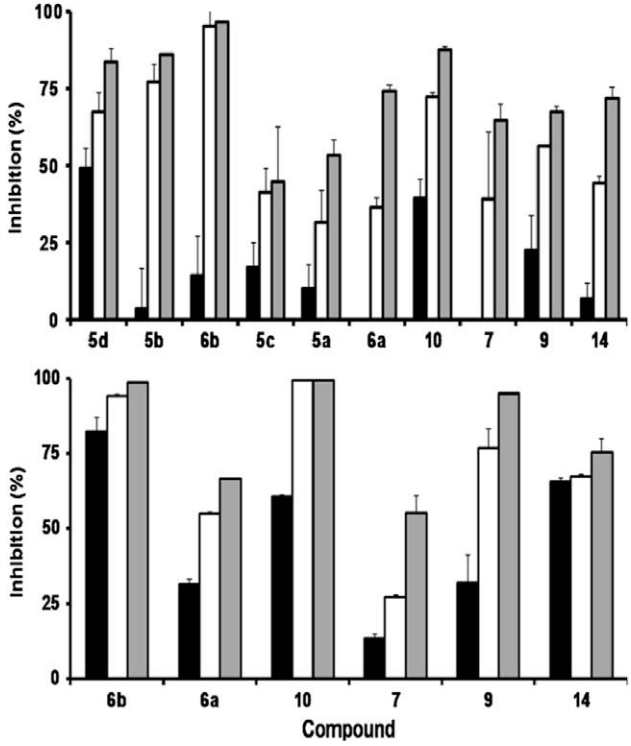

Figure 3. Rel protein inhibition by ppGpp analogues (shown in Schemes 1–3). Gray: 10 mM, white: 5 mM, black: 1 mM. (A) RelA. (B) Rel*seq*385.

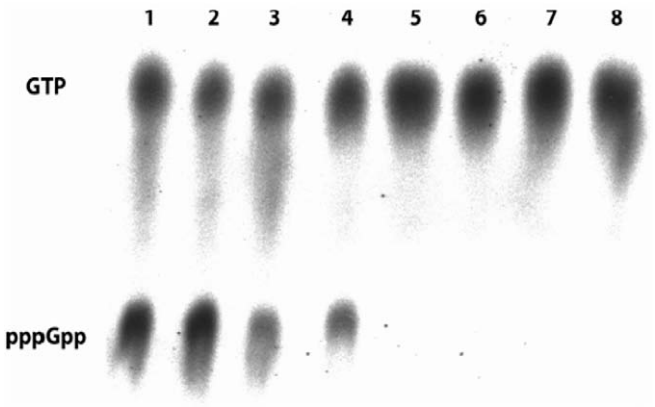

Figure 4. Inhibition of Rel-C638F by compound (**10**). Lanes 1–2: activity of Rel-C638F without compound (**10**); lanes 3–8: activity of Rel-C638F with increasing concentrations of compound (**10**); lanes 3–4: 1 mM; lanes 5–6: 5 mM and lanes 7–8: 10 mM.

compounds. Among compounds (**5d**), (**5b**), and (**6b**), the less bulky the substituent is, the more potent the inhibitory activity. When the 2′-hydroxyl is totally removed and replaced by a hydrogen atom (compound (**10**)), the highest levels of inhibition are observed. Also, substitution at the N^2 nitrogen of the guanine base reduces the inhibitory ability. On the other hand, compounds bearing only one bisphosphonate moiety at position 5′ (compounds (**7**) and (**9**)) or at position 3′ (compound (**14**)) show relatively moderate levels of inhibition. The same tendency is seen for the inhibition of Rel*seq*385 by the selected analogues (Fig. 3B).

Even though compound (**6b**) shows stronger activity at higher concentrations (5 and 10 mM), compound (**10**) was selected for further investigation as it was more potent at lower concentrations.

Since the ribosome-independent Rel*seq*385 was strongly inhibited by compound (**10**), we wanted to examine whether a ribosome-independent mutant of RelA, namely Rel-C638F,[32] could also be inhibited. As shown in Figure 4, compound (**10**) indeed inhibited the synthetic activity of Rel-C638F in vitro.

Attempting to explain the rapid accumulation of high levels of ppGpp during amino-acid starvation, Wendrich et al.[17] proposed a model suggesting that RelA is able to 'hop' between ribosomes as a consequence of (p)ppGpp synthesis.

Based on this model, we hypothesized that inhibition of (p)ppGpp synthesis would slow down RelA dissociation from the ribosome. In order to provide evidence of such an hypothesis, the amount of RelA proteins bound to the ribosome was quantified following the addition of increasing concentrations of compound (**10**) (Fig. 5). As clearly seen, lowering the levels of (p)ppGpp produced by RelA resulted in a remarkable decrease in RelA's ability to dissociate from the ribosome. The amount of bound protein (RelA) was increased up to threefold. Another protein tested was Rel-G251E, a RelA variant unable to synthesize (p)ppGpp.[32] In this case, the addition of increasing concentrations of compound (**10**) did not affect the dissociation of Rel-G251E from the ribosome.

The mutant *E. coli* strain *relC*, carrying a mutation in the structural gene for the ribosomal protein L11 (*rplK*), presents a relaxed phenotype under amino-acid starvation conditions.[33] RelA dissociation from ribosomes of *relC* was also examined (Fig. 5). It was evident that the addition of compound (**10**) did not affect the dissociation of RelA from L11 mutated ribosomes.

These data reinforce the notion that (p)ppGpp plays an important role in the dissociation of RelA from the ribosome.

In order to assess the inhibitory effect of compound (**10**) in greater detail, its capability to inhibit the synthetic activity of Rel*seq*385 and RelA was tested using a wider range of concentrations (0.1–10 mM). It was found that compound (**10**) inhibits (p)ppGpp accumulation by Rel*seq*385 even at concentrations as low as 0.2 mM (Fig. 6A). The compound exerted more than 50% inhibition of Rel*seq*385 at 0.5 mM, while more than 1 mM was needed in order to reach a similar level of RelA inhibition (Fig. 6B). Lowering the concentrations of compound (**10**) to submillimolar concentrations did not affect the in vitro accumulation of (p)ppGpp by RelA.

2.3. Compound (10) competes with GTP for its binding site

Based on the fact that compound (**10**) is able to inhibit both ribosome-dependent and independent Rel enzymes, it was assumed that the inhibitory mechanism through which the accumulation of (p)ppGpp is affected involves a direct inhibitor–enzyme interaction. As compound (**10**) inhibited both monofunctional RelA and bifunctional Rel*seq*385, the interaction was suspected to take place at the catalytic synthetase site of the two enzymes. To support this idea, the influence of the natural substrates of Rel proteins (GTP and ATP) on the inhibitory effect of compound (**10**) was tested. In vitro accumulation of (p)ppGpp via both ribosome-dependent (RelA) and ribosome-independent (Rel*seq*385) enzymes was measured in the presence of a constant concentration of compound (**10**) with increasing concentrations of either GTP or ATP. Figure 7A shows the influence of GTP on the inhibiton of RelA by compound (**10**). A distinct reversed linear correlation between the inhibitory activity and the GTP concentration is observed ($R^2 = 0.909$). A similar tendency can be seen for Rel*seq*385, although linearity is less obvious ($R^2 = 0.708$) (Fig. 7B).

No such correlation was found while examining the influence of compound (**10**)'s activity with increasing levels of ATP (data not shown). This is in agreement with the crystal structure of Rel*seq*385, where GTP is found in the catalytic site while ATP is not.[27]

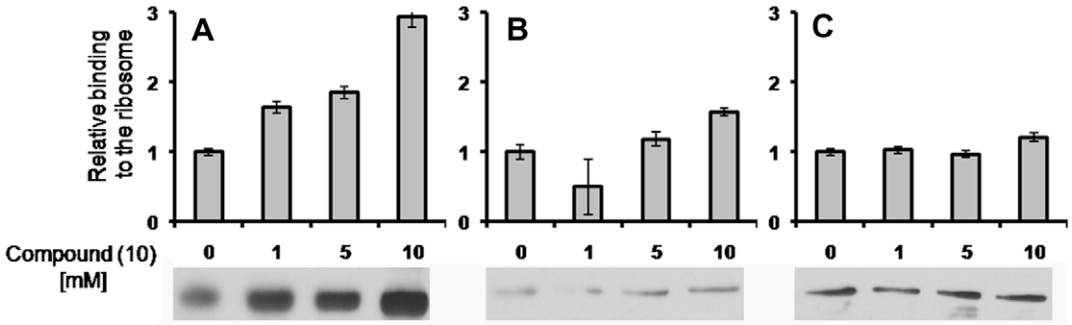

Figure 5. Compound (**10**) effect on the dissociation of RelA from the ribosome. Increasing amounts of compound (**10**) were added to in vitro reactions containing ribosomes and RelA (A) or Rel-G251E (B). (C) represents reactions where ribosomes produced from the mutant *E. coli* strain *relC* were used together with RelA.

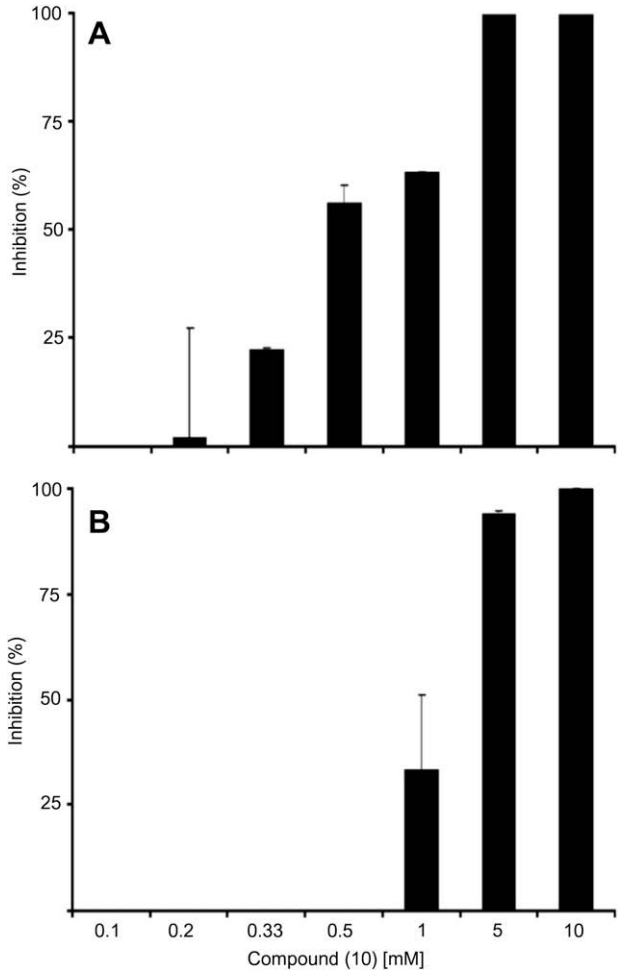

Figure 6. Inhibition by compound (**10**). (A) Rel*seq*385; (B) RelA.

These results strengthen the hypothesis that the inhibitor interacts with the enzyme at the catalytic synthetase site. Moreover, a direct competition between the inhibitor and GTP for the same binding site is likely. However, we have to keep in mind that the bifunctional Rel*seq*385 has two active sites that can accommodate (p)ppGpp and potentially its analogues: (1) the synthetase site where (p)ppGpp is the product of the reaction between GDP (GTP) and ATP and (2) the hydrolase site, where (p)ppGpp is the substrate, yielding GDP (GTP) and pyrophosphate. To examine the possible binding modes, we employed automated docking of compound (**10**) to both of these sites, each in its ON and OFF conformations.[27]

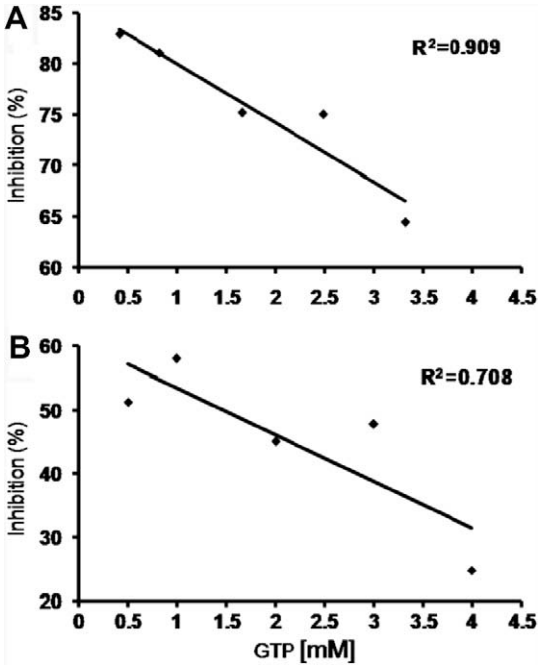

Figure 7. Rel protein inhibition by 5 mM of compound (**10**) in the presence of increasing concentrations of GTP. (A) RelA; (B) Rel*seq*385.

2.4. Prediction of the binding mode of compound (10)

Using the crystal structure of Rel*seq*385,[27] in silico docking of compound (**10**) into the catalytic synthetase site of the enzyme was initially carried out. Detailed analysis of key interactions of compound (**10**) and amino-acid residues of the (p)ppGpp-synthetase site resulted in the identification of a putative binding mode of compound (**10**) (Fig. 8). Interactions of GDP and Rel*seq*385 identified by X-ray crystallography[27] were used as constraints for the docking of compound (**10**). Based on experimental results, it is very likely that the guanine moiety of compound (**10**) binds to Rel*seq*385 in a similar way as observed for GDP. Therefore, the hydrogen bond between the backbone carbonyl of Ala335 of Rel*seq*385 and N1 of compound (**10**) as well as the one between the side-chain amide of Asn306 of Rel*seq*385 and O6 of compound (**10**) were used as constraints for docking. Compound (**10**) was docked into the synthetase active site of Rel*seq*385 in both the synthetase-ON and synthetase-OFF conformations as observed in the crystal structure.[27]

Interestingly, docking solutions obtained for the synthetase-ON site show that the 5′-bisphosphonate of compound (**10**) likely

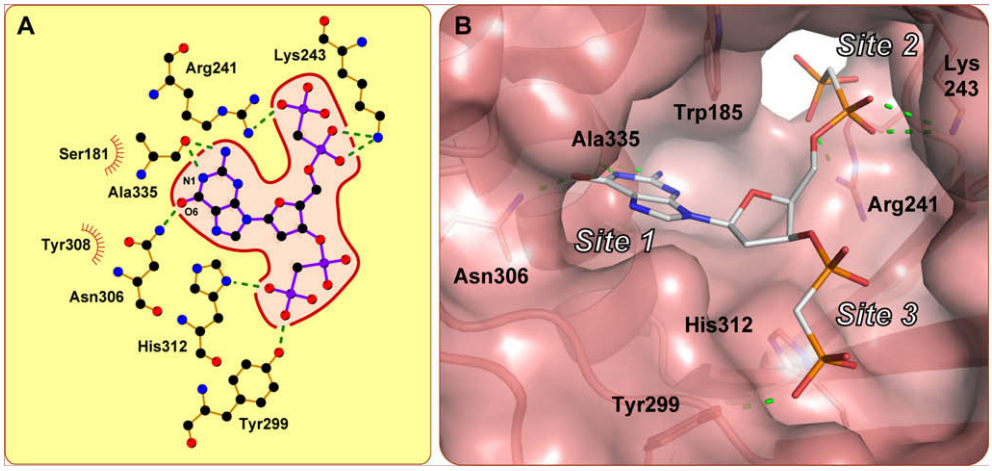

Figure 8. Predicted binding mode of compound (**10**) in the synthetase active site of Rel*seq*385 (synthetase-ON conformation) by automatic docking. (A) 2D-representation of the interactions between compound (**10**) and Rel*seq*385. Hydrogen bonds shown as dotted lines, van-der-Waals interactions as half-circles. (B) Surface representation of the synthetase active site (brown) with compound (**10**) shown as sticks with atoms colored as follows: carbon—gray, oxygen—red, nitrogen—blue, phosphorus—orange.

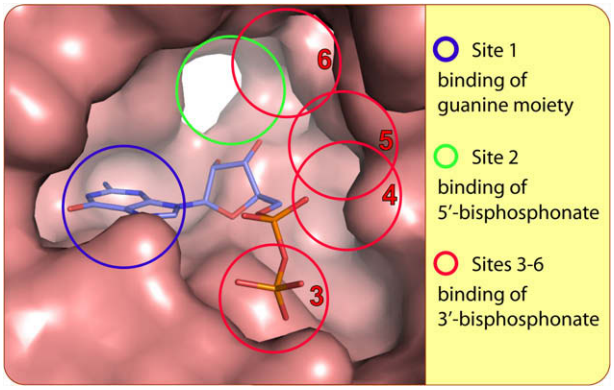

Figure 9. Overview of predicted binding sites for compound (**10**) in the synthetase-ON active site of Rel*seq*385, based on the top-ten solutions obtained from automated docking. Surface representation of the synthetase active site (brown), positions of binding site 1 (blue), site 2 (green), and alternative sites 3–6 (red) shown as circles. GDP (carbons—blue, heteroatoms colored as in Fig. 8B) from the crystal structure of Rel*seq*385 is shown for orientation.

binds to a unique, positively charged subpocket (Site 2) next to Site 1 (Fig. 8). All docking solutions show an orientation of the 5′-bisphosphonate that is different from the orientations found for the 5′-diphosphate of GDP in the synthetase-ON and -OFF states of Rel*seq*385 in the crystal structure. The interaction is stabilized by hydrogen bonding and polar contacts with Arg241, Lys243, Ser247, His244 and Trp185. An inspection of the top-ten docking solutions showed that the 3′-bisphosphonate moiety of compound (**10**) most probably adopts the conformation shown in Figure 8. This conformation was found in three of the top-ten docking solutions. Still, scoring results are very similar among the top-ten solutions (GOLD fitness score 93 for the best solution and 84 for the solution ranked number 10). Taking all top-ten solutions into account, there are four distinct potential interaction sites for the 3′-bisphosphonate group of compound (**10**) (Fig. 9; Sites 3–6). This result might reflect possible alternative binding modes of this moiety. One binding mode shows a similar orientation of the 3′-bisphosphonate of compound (**10**) and the 5′-diphosphate of GDP (Site 3; Fig. 9). In contrast, compound (**10**) does not seem to possess high binding affinity for the synthetase active site in the OFF conformation. In this conformation, Rel*seq*385 lacks a well-defined Site 2 and is therefore unable to accommodate the 5′-bisphosphonate moiety. This is reflected in low docking scores, showing a reduction by more than 50% compared to solutions for the synthetase site in the ON conformation. Solutions obtained show unfavorable van-der-Waals clashes between compound (**10**) and the more restricted synthetase site in the OFF conformation.

The crystal structure of Rel*seq*385 suggests that intramolecular crosstalk between synthetase and hydrolase domains regulate the activity of the two opposing catalytic sites. To avoid futile cycling of synthesis and hydrolysis of (p)ppGpp, nucleotide binding in the synthetase-ON state leads to conformational changes that switch off the hydrolase activity and vice versa. The inhibitory effect of non-reactive ATP analogues (ApNHpp or $ApCH_2pp$) on both synthetase and hydrolase activity of Rel*seq*385 provided further evidence for this reciprocal regulation mechanism.[27] It is therefore possible that the observed inhibitory effect of compound (**10**) on (p)ppGpp synthesis is the result of a binding event in the hydrolase site of Rel*seq*385, leading to allosteric signaling and subsequent inactivation of the synthetase site. Indeed, docking studies revealed that compound (**10**) is able to bind to the hydrolase site of Rel*seq*385 (as does the substrate of that site, (p)ppGpp). In all solutions identified, the 3′- or 5′-bisphosphonate groups of compound (**10**) participate in the coordination of the Mn^{2+} ion located in the hydrolase site, whereas multiple orientations were obtained for the guanine and ribose moieties. Although the docking results should be interpreted with caution, slightly higher scores for the best docking solution for the hydrolase-ON conformation compared to the best solution for the hydrolase-OFF conformation of the enzyme might indicate an increased affinity of compound (**10**) to this state of Rel*seq*385.

Our results from the docking studies provide a mechanistically plausible model of the inhibitor orientation in the ON conformation of the synthesis active site, whereas binding of the inhibitor to the synthesis site in the OFF conformation seems unlikely. Surprisingly, the 5′-bisphosphonate of compound (**10**) adopts a unique conformation strikingly different from the 5′-diphosphate of GDP in the crystal structure of Rel*seq*385. It binds to a deep, well-defined pocket of strong positive charge (Site 2) present only in the synthesis-ON conformation of Rel*seq*385. This site is well suited to accommodate phosphonate or phosphate moieties. In fact, in previous docking studies using ATP as a ligand, we predicted that during (p)ppGpp synthesis, the triphosphate of ATP might be located in Site 2 (data not shown). Therefore, the mode of action of compound (**10**) might provide means to block the binding of GTP and to interfere with the binding of ATP, both substrates needed

for (p)ppGpp synthesis. Although our docking studies together with results from competition experiments of compound (**10**) and GTP strongly suggest that compound (**10**) preferably binds to the synthetase active site of Rel*seq*385, we cannot rule out that additional interactions at the hydrolase site influence the synthetase activity by allosteric signaling. To assess if conformational crosstalk between hydrolase and synthetase plays a role in inhibition of Rel*seq*385 by compound (**10**), more experimental evidence is needed.

3. Conclusions

ppGpp analogues were synthesized and their inhibitory effects on Rel proteins from Gram-negative and Gram-positive bacteria were tested in vitro. It was found that both RelA and Rel*seq*385 were inhibited mostly by analogues bearing bisphosphonate groups at positions 5′ and 3′. Inhibition of Rel*seq*385 was more effective than that of RelA, either due to differences in the structure of the synthetase site, or additional binding of the compound to the Rel*seq*385 hydrolase site, thereby inhibiting the synthetase site through an allosteric effect.

An inverse correlation was found between the degree of inhibition of the synthetic activity of RelA and its dissociation from the ribosome.

It was shown that compound (**10**) competes with GTP but not with ATP. In silico docking studies with Rel*seq*385 suggest that this competition likely occurs at the binding pocket of GDP/GTP situated at the active site of the synthetase domain. The identification of distinct binding sites for all moieties of compound (**10**) will allow rational modification of the molecule to further improve properties important for efficient and selective inhibition of (p)ppGpp synthesis by Rel proteins.

By inhibiting the synthetic activity of Rel proteins, we may in fact prevent bacteria from sensing conditions where amino-acids are absent in their environment. This, in turn, may ultimately lead to bacterial self-starvation and death. In order to confirm these assumptions, bacterial uptake of negatively charged inhibitors is currently investigated at our laboratories.

Very recently, we succeeded in determining the crystal structure of Rel*seq*385 in complex with compound (**10**). Although this structure requires further refinement and improvement of resolution, it clearly shows that compound (**10**) binds exclusively to the synthetase catalytic site in its ON conformation. The binding mode seen in the crystals (at this stage of refinement) is very similar to the one shown in Figure 8. There is no large-scale conformational change of the protein visible, compared to our previous crystal structure of Rel*seq*385.[27]

4. Experimental

4.1. Materials

All chemicals and reagents were purchased from Sigma–Aldrich Ltd and used without further purification. Ultra-dry solvents stored with molecular sieves under an argon atmosphere were purchased from Acros Ltd. HPLC solvents were acquired from Bio-Lab Ltd. Radioactive α-^{32}P-GTP was purchased from Isotope Ltd.

4.2. NMR

NMR data were collected with a Varian VXR-300 MHz spectrometer equipped with a 5-mm switchable probe. Data were processed using the VNMR software. NMR abbreviations are as follows: s (singlet), d (doublet), t (triplet), q (quartet), m (multiplet), br (broad).

4.3. Mass spectrometry (HRMS)

Mass spectrometry was carried out with Orbi-trap (Thermo Finnigen) using nanospray attachment. MRFA was used as internal standard. Data were processed using BIOWORKS 3.3 package.

4.4. UV–vis spectrometry

UV–vis spectrophotometric data were collected with an Ultrospec 2100 Pro Spectrophotometer. Data were processed using the Swift II Wavescan™ software (Biochrom Ltd).

4.5. HPLC

Analytical HPLC was performed using a Shimadzu LC-2010 *HT* HPLC system equipped with a UV detector using a Merck RP-C18 25 × 4.6-mm column. Preparative and semi-preparative chromatography fractions were collected on a SpectraSystem SCM 1000 HPLC system equipped with a Gilson 117 UV detector, using Phenomenex RP-C18 25 × 10-mm and 25 × 22-mm columns.

4.6. Inhibitor docking into the synthetase and hydrolase sites of Rel*seq*385

The crystal structure of Rel*seq*385[27] (pdb code: 1VJ7), which shows the protein in the synthetase-ON/hydrolase-OFF conformation (molecule A) and in the synthetase-OFF/hydrolase-ON conformation (molecule B), was used as a target for docking of compound (**10**). Atom types and protonation states were assigned using SYBYL (Tripos, St. Louis, MO, USA). For docking into the synthetase active site, hydrogen-bonding interactions between the guanine moiety of GDP and the protein in the crystal structure were introduced as constraints, assuming they would be preserved in the complex with compound (**10**). Docking calculations were performed using the program GOLD.[34] Docking solutions were ranked according to the internal scoring function implemented in GOLD.

4.7. Cell-growth media

The growth media used was Luria–Bertani (LB) (1.6% tryptone, 1% yeast extract, 0.5% NaCl). Antibiotics used for selections were added at the following concentrations: 100 μg of ampicillin/mL and 50 μg of kanamycin/mL.

4.8. Protein purification

Starter cultures of ΔrelA *E. coli* strain from our laboratory collection[32] over-expressing either pQE30-RelA (pQE30-XA (QIAGEN) carrying *E. coli* RelA) or pENH385 (pET-21(+) (Novagen) carrying Rel*seq*385[35]) were grown overnight at 37 °C with shaking. The next day, cultures were diluted 1:50 in 400 mL LB containing the proper antibiotic and cells were grown at 37 °C until they reached an OD_{600} = ~0.6. Then, isopropyl-β-thio-galactopyranoside (IPTG) (1 mg/mL) was added and the cells were grown at the same conditions for an additional 2–3 h. Subsequently, cells were harvested for 10 min at 4000 rpm and the pellet was frozen at −70 °C overnight. The pellet was resuspended in 20 mL of lysis buffer containing 0.5 M NaCl, 20 mM NaH_2PO_4 (pH 8) and 10 mM imidazole. Lysozyme was added to a final concentration of 3 mg/mL together with a tablet of protease-inhibitor cocktail (Complete™, EDTA-free; Roche) and the cells were then subjected to 3.5 min of sonication in order to break their outer membrane. The resuspended pellet was centrifuged at 10,000 rpm at 4 °C for 10 min to remove the broken membrane. A sample of the soluble fraction was taken and the supernatant was gently mixed with Ni-NTA beads (QIAGEN) at 4 °C for 1 h. The beads were loaded onto a column and washed

with 50 mL of washing buffer containing 0.5 M NaCl, 20 mM NaH_2PO_4 (pH 8) and 20 mM imidazole and a sample was taken. Elution of the bound protein was achieved by the addition of 30 mL of elution buffer, containing 0.5 M NaCl, 20 mM NaH_2PO_4 (pH 8) and 250 mM imidazole. The elution fractions were run on a 12% acrylamide/bisacrylamide gel and the fractions containing the highest amount of protein were loaded onto a cellulose tubular membrane, mwco 12,000–14,000 (Cellu Sep), and stirred in dialysis buffer containing 100 mM Tris–acetate (pH 8.5), 10 mM EDTA, 1 mM DTT and 25% glycerol (two times overnight at 4 °C). After dialysis, the concentration of the purified proteins was determined using Bradford reagent (OD_{595}).

4.9. Ribosome preparation

Ribosomes were prepared as described by Block and Haseltine[36] with the following modifications: cells were grown in LB medium with shaking at 37 °C. At an OD_{600} of 1.5, 2 L of the cell culture was pelleted at 4 °C (6000 rpm for 20 min) and frozen overnight at −70 °C. Next, the pellet was resuspended in 60 mL of cold ribosome buffer containing 100 mM Tris–acetate (pH 8.0), 10 mM $Mg(OAc)_2$, and 1 mM dithiothreitol. Lysozyme was added to a final concentration of 3 mg/mL together with a tablet of protease-inhibitor cocktail (Complete™, EDTA-free; Roche), and cells were lysed by vigorous vortexing. Cells were then sonicated on ice for 3.5 min and pelleted at 4 °C (15,000 rpm for 40 min). A sample of the supernatant representing the soluble proteins before fractionation was saved for further analysis, while the rest of the supernatant was centrifuged in a Beckman Ti-65 rotor (30,000 rpm) at 4 °C for 4 h. The pellet was dissolved and kept stirred at 4 °C in 10 mL of ribosome buffer overnight. On the following day, the supernatant was pelleted at 10,000 rpm at 4 °C for 15 min in order to remove excess membrane residues and stored on ice. A ribosome buffer containing 40% sucrose was prepared and 5 mL were loaded into 30 mL polycarbonate Ultra bottles (Sorvall Instruments). Thereafter, the supernatant was loaded on top of the sucrose buffer and the bottles were centrifuged using a Beckman Ti-65 rotor (32,000 rpm) at 4 °C for 4 h.

The pellet was then suspended in 2 mL of ribosome buffer and the ribosomes were frozen and stored at −70 °C. Protein concentrations in the ribosomal fraction were determined based on RNA measurements in an ND-1000 Spectrophotometer (Nano-Drop).

4.10. In vitro (p)ppGpp accumulation assay

5× reaction mixture containing 2.5 mM GTP, 20 mM ATP, 200 mM Tris–HCl (pH 7.4), 5 mM DTT, 50 mM $MgCl_2$, 50 mM KCl, 135 mM $(NH_4)_2SO_4$ and α-^{32}P-GTP (0.1 μL per reaction) was freshly prepared. 0.5–1 μg of either RelA or Rel*seq*385 together with 1× reaction mixture and 30 μg of ribosomes (where necessary) were mixed in a total volume of 20 μL. Each reaction also contained a ppGpp analogue at a concentration ranging between 0 and 10 mM. The reactions were incubated at room temperature for a period of either 5 min (Rel*seq*385) or 60 min (RelA). The reactions were stopped by the addition of 5 μL formic acid. Five microliters of each reaction were loaded onto Cellulose PEI (Merck) and run for 2 h in 1.5 M KH_2PO_4. The data was analyzed using image reader 1000 V1.8 and the (p)ppGpp content was determined using the TINA 2.0 software (Raytest, Strauben-Hardt, Germany).

4.11. Measurements of dissociation of Rel proteins from ribosomes

In vitro reactions were carried on as mentioned above, but without the presence of labeled ^{32}P-GTP with increasing concentrations of compound (**10**) added. The reactions were then centrifuged for 4 h at 32,000 rpm at 4 °C and each reaction was divided into two fractions: soluble or ribosomal. The ribosomal samples were separated by 12% SDS–polyacrylamide gel electrophoresis, transferred to a PVDF membrane (Millipore, Bedford, MA), and processed for immunoreaction using anti-His antibodies (1:10,000, GE Healthcare). Immunoreactive proteins were detected using a chemiluminescence kit (Biological Industries, Bet Haemek, Israel) according to manufacturer's protocol and quantified using the TINA 2.0 software (Raytest, Strauben-Hardt, Germany).

4.12. Chemical synthesis

4.12.1. N^2-Isobutyrylguanosine (1)

Guanosine hydrate (10 g, 35.3 mmol) was dried by co-evaporating its suspension in dry pyridine (3 × 100 mL). The residue was suspended in dry pyridine (250 mL) under nitrogen atmosphere, and chlorotrimethylsilane (28.8 g, 265 mmol) was added. The reaction mixture was stirred at ambient temperature for 2 h, cooled to 0 °C, and isobutyryl chloride (11.3 g, 106 mmol) was added dropwise over 20 min. The mixture was allowed to warm to room temperature and stirred for 3 h. The reaction mixture was cooled to 0 °C and quenched by addition of H_2O (30 mL). After stirring for 5 min at 0 °C and 5 min at room temperature, concentrated aqueous NH_4OH (65 mL) was added. The solution was stirred for an additional 15 min at room temperature. The mixture was diluted with H_2O (500 mL) and washed with DCM (200 mL). The aqueous layer was concentrated by evaporation and the residue was recrystallized from hot H_2O to afford N^2-isobutyryl guanosine (9.90 g, 79%) as a white solid.

HRMS: Calcd: 354.1408. Found: 354.1404.

^{1}H NMR (300 MHz, D_2O-*d*): 8.10 (s, H8), 5.90 (d, *J* = 4.7 Hz, H1′), 4.68 (t, *J* = 5.0 Hz, H2′), 4.45 (t, *J* = 5 Hz, H3′), 3.95 (m, H4′), 3.86 (m, *J* = 12 Hz, H5′ H5″), 2.77 (m, 1H (*i*bu)), 1.25 (d, 6H, *J* = 6.8 Hz, (*i*bu)).

4.12.2. N^2-Isobutyryl-5′-*O*-dimethoxytrityl guanosine (2)

Compound (**1**) was dried three times by co-evaporation with dry pyridine. To a stirred suspension of dry N^2-isobutyryl guanosine (5 g; 14.15 mmol) in pyridine (100 mL), a solution of dimethoxytrityl chloride (5 g; 14.8 mmol) in pyridine (30 mL) was added dropwise over a period of 60 min. The reaction mixture was stirred for 4 h at room temperature, cooled to 0 °C by immersion in an ice/water bath, quenched with 5% $NaHCO_3$ (100 mL), and extracted with ethyl acetate (3 × 100 mL). The organic layers were combined, dried over magnesium sulfate, concentrated in vacuum and the residue was co-evaporated with toluene. The gum oil residue was dissolved in a minimum amount of DCM and added dropwise to a mixture of diethyl ether and petroleum ether (2000 mL 3:1) while stirring. Pure N^2-isobutyryl-5′-*O*-dimethoxytrityl guanosine precipitated from the solution, collected by filtration and dried to obtain a white powder. Yield: 75%.

HRMS: Calcd: 656.2714. Found: 656.2713.

^{1}H NMR (300 MHz, DMSO-*d*): 8.10 (s, H8), 7.0–7.6 (m, 13H, aromatic DMT), 5.82 (d, *J* = 7, H1′), 5.48 (d, *J* = 5.6, OH 2′), 5.18 (d, *J* = 5.6, OH 3′), 4.54–4.49 (q, *J* = 14.6 Hz, H2′), 4.22–4.17 (q, *J* = 15.5, H3′), 4.08–4.06 (q, *J* = 12 Hz, H4′), 3.82 (s, 6H, DMT–OCH_3), 3.2 (m, H5′ H5″), 2.75 (m, 1H (*i*bu)), 1.13 (d, *J* = 7 Hz, 6H (*i*bu)).

4.12.3. N^2-Isobutyryl-5′-*O*-dimethoxytrityl-2′(3′)-*O*-*tert*-butyldimethylsilyl guanosine (3a,b)

These compounds were prepared according to Sung et al.[28]

The crude isomers (2′-OTBDMS and 3′-OTBDMS) were separated using preparative RP-C18 HPLC, applying 70% acetonitrile in water as the mobile phase at a flow rate of 4 mL/min.

4.12.3.1. Compound (3a): N^2-Isobutyryl-5′-*O*-dimethoxytrityl-3′-*O*-*tert*-butyldimethylsilyl guanosine. White powder. Yield: 34%.

HRMS: Calcd: 770.3579. Found: 770.3577.

^{1}H NMR (300 MHz, DMSO-*d*): 8.10 (s, H8), 7.0–7.6 (m, 13H, aromatic DMT), 5.85 (d, *J* = 6.1 Hz, H1′), 5.11 (d, *J* = 6.3 Hz, OH 2′), 4.63–4.6 (q, *J* = 17.1 Hz, H2′), 4.23–4.21 (t, *J* = 8 Hz, H3′), 3.95–3.93 (q, *J* = 12 Hz, H4′), 3.78 (s, 6H, DMT–OCH_3), 3.2–3.4 (m, H5′ H5″), 2.78 (m, 1H (*i*bu)), 1.10 (d, *J* = 7 Hz, 6H (*i*bu)), 0.83 (s, 9H, *t*Bu–Si), 0.02 (s, 6H, $(CH_3)_2$–Si).

4.12.3.2. Compound (3b): N^2-Isobutyryl-5′-*O*-dimethoxytrityl-2′-*O*-*tert*-butyldimethylsilyl guanosine. White powder. Yield: 63%.

HRMS: Calcd: 770.3579. Found: 770.3573.

^{1}H NMR (300 MHz, DMSO-*d*): 8.12 (s, H8), 7.1–7.7 (m, 13H, aromatic DMT), 5.88 (d, *J* = 5.8 Hz, H1′), 5.48 (d, *J* = 5.4 Hz, OH 3′), 4.6 (t, *J* = 10.7 Hz, H2′), 4.17–4.14 (q, *J* = 14.2 Hz, H3′), 4.08–4.06 (q, *J* = 11.7 Hz, H4′), 3.82 (s, 6H, DMT–OCH_3), 3.1–3.3 (m, H5′ H5″), 2.75 (m, 1H (*i*bu)), 1.13 (d, *J* = 7 Hz, 6H (*i*bu)), 0.87 (s, 9H, *t*Bu–Si), 0.03 (s, 6H, $(CH_3)_2$–Si).

4.12.4. N^2-Isobutyryl-2′(3′)O-*tert*-butyldimethylsilyl guanosine (4a,b)

1 g of (**3a** or **3b**) was dissolved in a solution of 5% dichloroacetic acid in dry CH_2Cl_2 (20 mL). After stirring for 15 min, the solvent was evaporated and the resulting oily residue was subjected to silica-gel column chromatography. The elution was conducted with CH_2Cl_2/MeOH (93:7 v/v). The appropriate fractions were pooled and concentrated to give pure (**4a**–**b**) as a white powder.

4.12.4.1. Compound (4a): N^2-Isobutyryl-3′-*O*-*tert*-butyldimethylsilyl guanosine. White powder. Yield: 90%.

HRMS: Calcd: 468.2272. Found: 468.2273.

^{1}H NMR (300 MHz, DMSO-*d*): 8.12 (s, H8), 5.88 (d, *J* = 5.8 Hz, H1′), 5.48 (d, *J* = 6.3 Hz, OH 2′), 5.31 (q, *J* = 14.3 Hz, H2′), 5.15 (t, *J* = 11.5 Hz, OH 5′), 4.57 (t, *J* = 8 Hz, H3′), 3.95 (m, H4′), 3.60–3.72 (m, H5′ H5″), 2.75 (m, 1H (*i*bu)), 1.13 (d, *J* = 7 Hz, 6H (*i*bu)), 0.87 (s, 9H, *t*Bu–Si), 0.03 (s, 6H, $(CH_3)_2$–Si).

4.12.4.2. Compound (4b): N^2-Isobutyryl-2′-*O*-*tert*-butyldimethylsilyl guanosine. White powder. Yield: 92%.

HRMS: Calcd: 468.2272. Found: 468.2272.

^{1}H NMR (300 MHz, DMSO-*d*): 8.10 (s, H8), 5.85 (d, *J* = 5.8 Hz, H1′), 5.15 (t, *J* = 11.5 Hz, OH 5′), 5.11 (d, *J* = 6.3 Hz, OH 3′), 4.72 (m, H2′), 4.2 (m, H3′), 4.09 (m, H4′), 3.2–3.4 (m, H5′ H5″), 2.78 (m, 1H (*i*bu)), 1.10 (d, *J* = 7 Hz, 6H (*i*bu)), 0.83 (s, 9H, *t*Bu–Si), 0.02 (s, 6H, $(CH_3)_2$–Si).

4.12.5. 2′,3′-Isopropylideneguanosine (8)

To a suspension of guanosine (5 g, 17 mmol) in 300 mL of acetone 70% perchloric acid (2 mL, 24 mmol) was added. After 70 min, concentrated ammonium hydroxide (3 mL, 25 mmol) was added to the reaction mixture and cooled down with an ice bath. The precipitate was filtered out and dried over vacuum. An off-white powder was obtained. Yield: 80%.

HRMS: Calcd: 324.1302. Found: 324.1304.

^{1}H NMR (300 MHz, DMSO-d_6): 10.67 (s, 1H, NH), 7.89 (s, H8), 6.50 (s, 2H, NH2), 5.90 (d, *J* = 5.8 Hz, H1′), 5.17 (t, *J* = 8.2 Hz, H2′), 5.03 (t, *J* = 11.5 Hz, OH 5′), 4.94 (t, *J* = 8 Hz, H3′), 4.09 (m, H4′), 3.50 (m, H5′ H5″), 1.49 (s, 3H, CH3), 1.29 (s, 3H, CH3).

4.13. General procedure for phosphonylation

The procedure was adapted from Kalek et al.,[29] as follows:

A solution of methylene bis-(phosphonic dichloride) (1.2 equiv for compounds (**7**) and (**9**) and 2.4 equiv for compounds (**5a**–**d**) and (**6a**–**b**)) in trimethyl phosphate (10 mL) cooled to 0 °C was added to a suspension of 1 equiv of an adequately protected nucleoside in trimethyl phosphate (10 mL) at 0 °C. The reaction mixture was stirred at 0 °C. After 20 h (2 h for compounds (**7**, **9**)), 0.5 M aqueous ammonium bicarbonate (pH 7.0) was added. Chromatographic purification was carried out first on HPLC DEAE–Sephadex, using a 0–1 M gradient of ammonium bicarbonate followed by RP-C18 HPLC, resulting in white powders after lyophilization.

4.13.1. Guanosine 5′-methylene bisphosphonate (7)

Starting material: guanosine, 70% yield.

HRMS: Calcd: 442.0523. Found: 442.0524.

^{1}H NMR (300 MHz, D_2O-*d*): 8.10 (s, H8), 5.90 (d, *J* = 5.8 Hz, H1′), 4.68 (t, *J* = 8.2 Hz, H2′), 4.45 (t, *J* = 8 Hz, H3′), 4.2 (m, H4′), 3.98 (m, H5′ H5″), 2.2 (t, P–CH_2–P).

^{31}P NMR (163 MHz): δ 19.15, 16.37.

4.13.2. 2′,3′-Isopropylideneguanosine-5′-methylene bisphosphonate) (9)

Starting material: (**8**), 67% yield.

HRMS: Calcd: 482.0836. Found: 482.0837.

^{1}H NMR (300 MHz, D_2O): 7.93 (s, 1H), 5.90 (d, *J* = 5.8 Hz, H1′), 5.17 (t, *J* = 8.2 Hz, H2′), 4.94 (t, *J* = 8 Hz, H3′), 4.09 (m, H4′), 3.80 (m, H5′ H5″), 2.3 (t, *J* = 19.8 Hz, P–CH_2–P), 1.49 (s, 3H, CH3), 1.29 (s, 3H, CH3).

^{31}P NMR (163 MHz): δ 18.2, 16.1.

4.13.3. N^2-Isobutyryl-guanosine-2′-5′-di(methylene bisphosphonate) (5a)

Starting material: (**4a**), 53% yield.

HRMS: Calcd: 670.0476. Found: 670.0477.

^{1}H NMR (300 MHz, D_2O): 8.12 (s, H8), 6.08 (d, *J* = 5.8 Hz, H1′), 5.31 (m, H2′), 4.57 (t, *J* = 8.9 Hz, H3′), 3.95 (m, H4′), 3.60–3.72 (m, H5′ H5″), 2.75 (m, 1H (*i*bu)), 2.1–2.3 (t, *J* = 19.7 Hz, P–CH_2–P), 1.13 (d, 6H (*i*bu)).

^{31}P NMR (163 MHz): δ 18.5, 18.2, 16.1, 15.8.

4.13.4. N^2-Isobutyryl-guanosine-3′-5′-di(methylene bisphosphonate) (5b)

Starting material: (**4b**), 44% yield.

HRMS: Calcd: 670.0476. Found: 670.0476.

^{1}H NMR (300 MHz, D_2O): 8.10 (s, H8), 5.85 (d, *J* = 5.8 Hz, H1′), 4.72 (t, *J* = 8 Hz, H2′), 4.2 (m, H3′), 4.09 (m, H4′), 3.5 (m, H5′ H5″), 2.78 (m, 1H (*i*bu)), 2.1 (t, *J* = 19.9 Hz, P–CH_2–P), 1.10 (d, 6H (*i*bu)).

^{31}P NMR (163 MHz): δ 19.1, 18.0, 16.1, 15.5.

4.13.5. N^2-Isobutyryl-3′-*O*-*tert*-butyldimethylsilyl-guanosine–2′-5′-di(methylene bisphosphonate) (5c)

Starting material: (**4a**), 9% yield.

HRMS: Calcd: 784.1340. Found: 784.1342.

^{1}H NMR (300 MHz, D_2O): 8.12 (s, H8), 5.92 (d, *J* = 5.8 Hz, H1′), 5.30 (m, H2′), 4.57 (t, *J* = 8 Hz, H3′), 3.95 (m, H4′), 3.60–3.72 (m, H5′ H5″), 2.75 (m, 1H (*i*bu)), 2.1–2.2 (t, *J* = 19.7 Hz, P–CH_2–P), 1.13 (d, 6H (*i*bu)), 0.87 (s, 9H, *t*Bu–Si), 0.03 (s, 6H, $(CH_3)_2$–Si).

^{31}P NMR (163 MHz): δ 18.8, 18.5, 16.2, 15.9.

4.13.6. N^2-Isobutyryl-2′-*O*-*tert*-butyldimethylsilyl guanosine-3′-5′-di(methylene bisphosphonate) (5d)

Starting material: (**4b**), 8% yield.

HRMS: Calcd: 784.1340. Found: 784.1336.

^{1}H NMR (300 MHz, D_2O): 8.15 (s, H8), 5.87 (d, *J* = 5.8 Hz, H1′), 4.75 (t, *J* = 8 Hz, H2′), 4.2 (m, H3′), 4.09 (m, H4′), 3.4 (m, H5′ H5″), 2.78 (m, 1H (*i*bu)), 2.0–2.2 (t, *J* = 19.9 Hz, P–CH_2–P), 1.10 (d, 6H (*i*bu)), 0.83 (s, 9H, *t*Bu–Si), 0.02 (s, 6H, $(CH_3)_2$–Si).

^{31}P NMR (163 MHz): δ 19.2, 18.6, 16.5, 16.1.

4.13.7. 2′-Deoxyguanosine-3′-5′-di(methylene bisphosphonate) (10)

Same procedure as used for preparing (**6a**) using 2′-deoxyguanosine as starting material. Yield: 73%.

HRMS: Calcd: 584.0108. Found: 584.0108.

^{1}H NMR (300 MHz, D_2O): 8.15 (s, H8), 5.80 (t, J = 13.4 Hz, H1′), 4.7 (m, H2′ H2″), 4.2 (m, H3′), 4.09 (m, H4′), 3.6 (m, H5′ H5″), 2.2 (t, J = 19.7 Hz, P–CH_2–P).

^{31}P NMR (163 MHz): δ 19.2, 18.3, 16.3, 15.9.

4.14. Guanosine-2′(3′)-5′-di(methylene bisphosphonate) (6a,b)

4.14.1. Guanosine-2′-5′-di(methylene bisphosphonate) (6a)

Compound (**5a**) was subjected to hydrolysis overnight at 60 °C in 25% ammonium hydroxide and was then lyophilized. The crude material was applied to a RP-C18 preparative column, applying 5 mM ammonium acetate in water as the mobile phase at a flow rate of 4 mL/min.

The desired product was obtained as a white powder. 88% yield.

HRMS: Calcd: 600.0057. Found: 600.0057.

^{1}H NMR (300 MHz, D_2O): 8.12 (s, H8), 5.88 (d, J = 5.8 Hz, H1′), 5.31 (m, H2′), 4.57 (t, J = 8.6 Hz, H3′), 3.95 (m, H4′), 3.72 (m, H5′ H5″), 2.2 (t, J = 19.8 Hz, P–CH_2–P).

^{31}P NMR (163 MHz): δ 18.9, 18.4, 16.0, 15.8.

4.14.2. Guanosine-3′-5′-di(methylene bisphosphonate) (6b)

Same procedure as used for preparing (**6a**) using (**5b**) as the starting material. White powder. 90% yield.

HRMS: Calcd: 600.0057. Found: 600.0058.

^{1}H NMR (300 MHz, D_2O): 8.0 (s, H8), 5.9 (d, J = 5.8 Hz, H1′), 4.72 (t, J = 8.6 Hz, H2′), 4.2 (m, H3′), 4.09 (m, H4′), 3.5 (m, H5′ H5″), 2.0 (t, J = 19.8 Hz, P–CH_2–P).

^{31}P NMR (163 MHz): δ 19.2, 18.3, 16.3, 15.9.

4.15. 3′-*O*-5′-*O*-Diacetyl-2′-deoxyguanosine (11)

2′-Deoxyguanosine hydrate was repeatedly co-evaporated with pyridine and suspended in dry pyridine (100 mL). Acetic anhydride (50 mL) was added and the mixture was stirred at room temperature for 45 min. The solution was evaporated under reduced pressure. Fifty milliliters of water were added to the oily residue. The white solid formed was filtered and dried over phosphorus pentoxide. Yield: 90%.

HRMS: Calcd: 352.1251. Found: 352.1253.

^{1}H NMR (300 MHz, DMSO-d_6): 10.67 (s, N^1), 7.91 (s, H8), 6.50 (s, 2H, N^2), 6.13 (t, J = 14.5 Hz, H-1′), 5.30 (m, H-3′), 4.29 (m, H-4′), 4.16 (m, 2H, H-5′), 2.95 (m, 1H, H-2′), 2.48 (m, 1H, H-2′), 2.08 and 2.04 (two s, 6H, 2$COCH_3$).

4.16. 5′-*O*-Acetyl-2′-deoxyguanosine (12)

Compound (**11**) (0.2 g, 0.57 mmol) was dissolved in 5 mL pyridine and treated with hydrazine hydrate (55 μL, 1.1 mmol) at room temperature for 20 h. Acetone (1 mL) was added to the reaction mixture and stirred for 30 min. Then the solvents were removed under vacuum and the residue was co-evaporated with acetone. The desired compound was isolated on a preparative RP-C18 HPLC column using a gradient of 0–90% acetonitrile in water over 50 min at a flow rate of 5 mL/min. 2D NMR was used to identify the resulting compounds.

White powder, yield: 47%.

HRMS: Calcd: 310.1146. Found: 310.1148.

^{1}H NMR (300 MHz, DMSO-d_6): 10.67 (s, N^1), 7.91 (s, H8), 6.50 (s, 2H, N^2), 6.13 (t, J = 14.5 Hz, H-1′), 5.44 (br s, 1H, 3′OH), 4.39 (m, 1H, H-3′), 4.29 (m, H-4′), 4.16 (m, 2H, H-5′), 2.95 (m, 1H, H-2′), 2.48 (m, 1H, H-2′), 2.08 and 2.04 (two s, 6H, 2$COCH_3$).

4.17. 5′-*O*-Acetyl-3′-methylene bisphosphonate-2′-deoxyguanosine (13)

A solution of methylene bis-(phosphonic dichloride) (1.2 equiv) in trimethyl phosphate (10 mL) cooled to 0 °C was added to a suspension of 1 equiv of compound (**12**) in trimethyl phosphate (10 mL) at 0 °C. The reaction mixture was stirred at 0 °C. After 20 h, 0.5 M aqueous ammonium bicarbonate (pH 7.0) was added. Purification was conducted on HPLC using a RP-C18 column, applying 5 mM ammonium acetate in water as the mobile phase at a flow rate of 4 mL/min resulting in white powder after lyophilization.

Yield: 67%.

HRMS: Calcd: 468.0680. Found: 468.0680.

^{1}H NMR (300 MHz, D_2O): 7.85 (s, 1H, H-8), 6.11 (t, J = 14.5 Hz, H-1′), 5.21 (m, H-3′), 4.2 (m, 2H, H-5′), 2.64 (m, 1H, H-2′), 2.32 (m, 1H, H-2′), 2.21 (t, J = 19.7 Hz, P–CH_2–P), 2.01 (s, 3H, $COCH_3$).

^{31}P NMR (163 Hz, D_2O): 18.4; 15.2.

4.18. 3′-Methylene bisphosphonate-2′-deoxyguanosine (14)

Compound (**13**) was dissolved in concentrated ammonium hydroxide and heated to 60 °C for 15 h. The ammonium hydroxide was removed in vacuum and the solid residue was re-dissolved in water and lyophilized. The resulting solid was purified by HPLC employing a preparative RP-C18 column, applying 5 mM ammonium acetate in water as the mobile phase at a flow rate of 4 mL/min.

White powder, yield: 91%.

HRMS: Calcd: 426.0574. Found: 426.0572.

^{1}H NMR (300 MHz, D_2O): 7.85 (s, 1H, H-8), 6.11 (t, J = 14.5 Hz, H-1′), 5.21 (m, H-3′), 4.2 (m, 2H, H-5′), 2.64 (m, 1H, H-2′), 2.32 (m, 1H, H-2′), 2.21 (t, J = 19.7 Hz, P–CH_2–P).

^{31}P NMR (163 Hz, D_2O): 18.5; 15.4.

Acknowledgments

This work was supported by grants from the German Israel Foundation (835/2004 and 835/2007) to J.K., R.H., and G.G. R.H. thanks the Fonds der Chemischen Industrie and the DFG Cluster of Excellence 'Inflammation at Interfaces' for continuous support.

References and notes

1. Lock, R. L.; Harry, E. J. *Nat. Rev. Drug Disc.* **2008**, *7*, 324.
2. Walsh, C. *Nat. Rev. Microbiol.* **2003**, *1*, 65.
3. Cashel, M.; Gentry, D. R.; Hernandez, V. H.; Vinella, D. The stringent response. In *Escherichia coli and Salmonella typhimurium Cellular and molecular biology*; ASM Press: Washington, DC, 1996.
4. Cashel, M.; Gallant, J. *Nature* **1969**, *221*, 838.
5. Cashel, M.; Lazzarini, R. A.; Kalbacher, B. *J. Chromatogr.* **1969**, *40*, 103.
6. Gentry, D. R.; Hernandez, V. J.; Nguyen, L. H.; Jensen, D. B.; Cashel, M. *J. Bacteriol.* **1993**, *175*, 7982.
7. Hammer, B. K.; Tateda, E. S.; Swanson, M. S. *Mol. Microbiol.* **2002**, *44*, 107.
8. Haralalka, S.; Nandi, S.; Bhadra, R. K. *J. Bacteriol.* **2003**, *185*, 4672.
9. Na, H. S.; Kim, H. J.; Lee, H. C.; Hong, Y.; Rhee, J. H.; Choy, H. E. *Vaccine* **2006**, *24*, 2027.
10. Nakanishi, N.; Abe, H.; Ogura, Y.; Hayashi, T.; Tashiro, K.; Kuhara, S.; Sugimoto, N.; Tobe, T. *Mol. Microbiol.* **2006**, *61*, 194.
11. Pizarro-Cerda, J.; Tedin, K. *Mol. Microbiol.* **2004**, *52*, 1827.
12. Taylor, C. M.; Beresford, M.; Epton, H. A.; Sigee, D. C.; Shama, G.; Andrew, P. W.; Roberts, I. S. *J. Bacteriol.* **2002**, *184*, 621.
13. Hesketh, A.; Chen, W. J.; Ryding, J.; Chang, S.; Bibb, M. *Genome Biol.* **2007**, *8*, R161.
14. Dahl, J. L.; Kraus, C. N.; Boshoff, H. I.; Doan, B.; Foley, K.; Avarbock, D.; Kaplan, G.; Mizrahi, V.; Rubin, H.; Barry, C. E., III *Proc. Natl. Acad. Sci. U.S.A.* **2003**, *100*, 10026.
15. Metzger, S.; Dror, I. B.; Aizenman, E.; Schreiber, G.; Toone, M.; Friesen, J. D.; Cashel, M.; Glaser, G. *J. Biol. Chem.* **1988**, *263*, 15699.
16. Pedersen, F. S.; Kjeldgaard, N. O. *Eur. J. Biochem.* **1977**, *76*, 91.
17. Wendrich, T. M.; Blaha, G.; Wilson, D. N.; Marahiel, M. A.; Nierhaus, K. H. *Mol. Cell.* **2002**, *10*, 779.
18. Battesti, A.; Bouveret, E. *Mol. Microbiol.* **2006**, *62*, 1048.

19. Spira, B.; Silberstein, N.; Yagil, E. *J. Bacteriol.* **1995**, *177*, 4053.
20. Vinella, D.; Albrecht, C.; Cashel, M.; D'Ari, R. *Mol. Microbiol.* **2005**, *56*, 958.
21. Metzger, S.; Sarubbi, E.; Glaser, G.; Cashel, M. *J. Biol. Chem.* **1989**, *264*, 9122.
22. Xiao, H.; Kalman, M.; Ikehara, K.; Zemel, S.; Glaser, G.; Cashel, M. *J. Biol. Chem.* **1991**, *266*, 5980.
23. Mechold, U.; Cashel, M.; Steiner, K.; Gentry, D.; Malke, H. *J. Bacteriol.* **1996**, *178*, 1401.
24. Mittenhuber, G. *J. Mol. Microbiol. Biotechnol.* **2001**, *3*, 585.
25. Wendrich, T. M.; Marahiel, M. A. *Mol. Microbiol.* **1997**, *26*, 65.
26. Nanamiya, H.; Kasai, K.; Nozawa, A.; Yun, C. S.; Narisawa, T.; Murakami, K.; Natori, Y.; Kawamura, F.; Tozawa, Y. *Mol. Microbiol.* **2008**, *67*, 291.
27. Hogg, T.; Mechold, U.; Malke, H.; Cashel, M.; Hilgenfeld, R. *Cell* **2004**, *117*, 57.
28. Sung, W. L.; Narang, S. A. *Can. J. Chem.-Rev. Can. Chim.* **1982**, *60*, 111.
29. Kalek, M.; Jemielity, J.; Stepinski, J.; Stolarski, R.; Darzynkiewicz, E. *Tetrahedron Lett.* **2005**, *46*, 2417.
30. Yoshikawa, M.; Kato, T.; Takenishi, T. *Bull. Chem. Soc. Jpn.* **1969**, *42*, 3505.
31. Ishido, Y.; Nakazaki, N.; Sakairi, N. *J. Chem. Soc., Perkin Trans. 1* **1979**, 2088.
32. Gropp, M.; Strausz, Y.; Gross, M.; Glaser, G. *J. Bacteriol.* **2001**, *183*, 570.
33. Yang, X.; Ishiguro, E. E. *J. Bacteriol.* **2001**, *183*, 6532.
34. Jones, G.; Willett, P.; Glen, R. C.; Leach, A. R.; Taylor, R. *J. Mol. Biol.* **1997**, *267*, 727.
35. Mechold, U.; Murphy, H.; Brown, L.; Cashel, M. *J. Bacteriol.* **2002**, *184*, 2878.
36. Block, R.; Haseltine, A. W. *J. Biol. Chem.* **1975**, *250*, 1212.